METRICA
METRology Institutional CAtalog

ISTITUTO NAZIONALE DI RICERCA METROLOGICA
Repository Istituzionale

Total risk of a false decision on conformity of an alloy due to measurement uncertainty and correlation of test results

This is the author's accepted version of the contribution published as:

Original
Total risk of a false decision on conformity of an alloy due to measurement uncertainty and correlation of test results / Kuselman, I., Pennecchi, F.R., da Silva, R.J.N.B., Hibbert, D.B., Anchutina, E.. - In: TALANTA. - ISSN 0039-9140. - 189:(2018), pp. 666-674. [10.1016/j.talanta.2018.07.049]

Availability:
This version is available at: 11696/59855 since: 2020-09-28T18:32:04Z

Publisher:
Elsevier

Published
DOI:10.1016/j.talanta.2018.07.049

Terms of use:

This article is made available under terms and conditions as specified in the corresponding bibliographic description in the repository

Publisher copyright
Institute of Physics Publishing Ltd (IOP)
IOP Publishing Ltd is not responsible for any errors or omissions in this version of the manuscript or any version derived from it. The Version of Record is available online at DOI indicated above

(Article begins on next page)

10 October 2026

*Revised Manuscript (clean copy)
Click here to view linked References

Total risk of a false decision on conformity of an alloy due to measurement uncertainty and correlation of test results

Ilya Kuselman[a,] *, Francesca R. Pennecchi[b] , Ricardo J. N. B. da Silva[c] , D. Brynn Hibbert[d], Elena Anchutina[e]

[a] Independent Consultant on Metrology, 4/6 Yarehim St., 7176419 Modiin, Israel

[b] Istituto Nazionale di Ricerca Metrologica (INRIM), Strada delle Cacce 91, 10135 Turin, Italy

[c] Centro de Química Estrutural, Faculdade de Ciências da Universidade de Lisboa, Edifício C8, Campo Grande, 1749-016 Lisboa, Portugal

[d] School of Chemistry, UNSW Sydney, Sydney NSW 2052, Australia

[e] JSC Ekaterinburg Non-Ferrous Metal Processing Plant (EZOCM), 131 Uspensky Avenue, Verhnjaja Pyshma, 624097 Sverdlovsk region, Russia

---

* Corresponding author.

E-mail address: ilya.kuselman@bezeqint.net (I. Kuselman)

Tel.: +972-50-6240466

4/6 Yarehim St., Modiin, 7176419 Israel

ABSTRACT

Total risk (probability) of a false decision on conformity of an alloy due to measurement uncertainty and correlation of test results is quantified. As an example, a dataset of test results of a PtRh alloy is studied when contents of four components of the alloy composition are under control. There are specification limits for contents of 1) Pt and 2) Rh; 3) three precious impurities - Au, Ir and Pd, and 4) eight impurities, both precious Au, Ir, Pd, and non-precious Fe, Pb, Si, Sn, Zn. Test results of 100 batches of the alloy produced at the same plant, obtained by X-ray fluorescence and optical atomic emission spectrometry methods at the plant laboratory, were in the dataset. The Pt content was tested based on the mass balance. Measurement uncertainties of the test results are estimated summarizing data of validation reports of the measurement procedures for different elements/analytes. These test results are correlated because of the natural chemical origin of the raw materials used in the alloy production and mass balance constraints. Correlations between test results for two pairs of the components (Pt vs. Rh, and the three vs. the eight impurities) were strong. To assess the correlation effects on the total risk, the study was performed for two scenarios considering 1) correlated test results for all four components, and 2) practically uncorrelated test results for two components only - Rh and the eight impurities. A matrix Bayesian approach was applied for total risk evaluation, where the observed correlations are taken into account within the experimental correlation matrix. This matrix influenced all subsequent multivariate calculation results. It was shown that simplification of the testing by reducing the number of components under control leads to a significant increase of the probability of a false decision on conformity of an alloy batch randomly drawn from a statistical population of such batches. Core of the developed R code, used for the risk calculations, is presented.

Keywords:

Conformity assessment; Metals and alloys; PtRh composition; Measurement uncertainty; Correlated test results; Risk of false decisions

1. Introduction

Standard specifications for the chemical composition of an alloy limit the actual ('true') content c_i of the *i*-th component, $i = 1, 2, \ldots, n$, including base components, impurities or groups of impurities ('content' vs. 'concentration' is discussed in refs [1-3]). Conformity assessment of an alloy batch is based on comparing the content measurement/test results $c_{i\mathrm{m}}$ with such specification limits [4, 5]. Since any $c_{i\mathrm{m}}$ value has an associated measurement uncertainty [6], several kinds of risk of a false decision on conformity of a batch may be defined. The probability of accepting a batch of the alloy when it should have been rejected is named 'consumer's risk', whereas the probability of falsely rejecting the batch is the 'producer's risk'. For a specified batch, they are referred to as the 'specific consumer's risk' and the 'specific producer's risk' R_{ci}^{*} for the *i*-th particular component of the alloy under control. The risks of incorrect conformity assessment of a batch randomly drawn from a statistical population of such batches are the 'global consumer's risk' and the 'global producer's risk' R_{ci}, as they characterize the material production globally [7].

Conformity of a product is assessed before it is placed on the market. Bodies that protect the consumer, e.g. the European Commission, would like to ensure that non-compliant products do not find their way to the market [8]. Therefore, conformity assessment of each manufactured alloy batch is performed at the plant by the producer, before selling the batch. Deciding whether an alloy is conforming or not, the producer should minimize the consumer's risks. However, there is not a producer for whom the expenditure on production is not important. Thus, the producer's risks should be also evaluated and controlled at the plant.

An alloy is a multicomponent material, and in general a component-by-component evaluation of the risks of its conformity assessment is not complete, as this approach does not give an answer to the question of the probability of a false decision on conformity of the alloy as a whole. When conformity assessment for each *i*-th component of an alloy is successful (i.e. the particular specific R_{ci}^{*} or global R_{ci} risks are small enough), the total probability of a false decision concerning the alloy as a whole (the *total* specific R_{total}^{*} or *total* global R_{total} risk) might still be significant [9]. Using the law of total probability relating marginal probabilities to conditional probabilities, the total risk can be evaluated as a combination of the particular risks

whenever the variables (actual component content values c_i, and corresponding test results c_{im}) are independent. When the number n of components of the same material under control increases, the total risk also increases [10, 11].

Evaluating total risk for correlated quantities has been discussed in our paper [12], where specification limits of the active components' contents in tablets of a multicomponent medication were interpreted as a multivariate specification domain. Actual values of components' contents and corresponding test results were modelled by multivariate distributions, and the total global risk of a false decision on the material conformity was evaluated based on calculation of integrals of their joint probability density function. A total specific risk was evaluated as the joint posterior cumulative function of actual values of a specific batch lying outside the multivariate specification domain, when the vector of test results, obtained for the batch, is completely inside this domain. It was shown that the influence of correlation on the risk is not easily predictable.

The aim of the present paper is implementation of modelling and calculation of the total risks in conformity assessment of an alloy as a multicomponent material with a complex nature of correlation among contents of components. As an example, the risks in conformity of a PtRh alloy (CAS No. 11107-71-4) due to measurement uncertainty are quantified when four components of the alloy composition are under control (n = 4) and strong correlations among test results are observed. Quantification of these risks can be important for understanding quality of such alloys, which are widely used in thermocouples for temperature measurements; for oxidation catalysts, in particular, automobile catalytic converters; in electronics; glass industry; optics; as well as for the manufacture of jewelry [13].

A matrix Bayesian approach is applied for total risk evaluation [12], where the observed correlations are taken into account within the experimental correlation matrix. This matrix influenced all subsequent multivariate calculation results.

2. Material and test methods

Test results of a total N = 100 batches of PtRh 92.5-7.5 alloy for catalytic systems [14], produced during about two years at the same plant [15], were used as an example of a dataset for quantification of the total risks. The testing was performed at the plant laboratory for conformity assessment of the alloy batches to the standard [14].

2.1. Specification and acceptance limits

The standard [14] sets the lower and upper specification (tolerance [7]) limits, T_{Li} and T_{Ui}, of contents c_i of the four following components in PtRh 92.5-7.5 alloy:

i = 1) Pt content c_1 as mass fraction, $T_{L1} = 92.2\ \% \leq c_1 \leq 92.8\ \% = T_{U1}$;

i = 2) Rh content c_2 as mass fraction, $T_{L2} = 7.3\ \% \leq c_2 \leq 7.7\ \% = T_{U2}$;

i = 3) content c_3 of three precious impurities - Au, Ir and Pd - as sum of mass fractions, $c_3 \leq 0.12\ \% = T_{U3}$;

i = 4) content c_4 of eight impurities, both precious Au, Ir and Pd and non-precious Fe, Pb, Si, Sn and Zn, as sum of mass fractions, $c_4 \leq 0.18\ \% = T_{U4}$.

Limitation of the impurities' contents, which assure the alloy purity, prevents a change of its microstructure influencing high-temperature resistance, catalytic and other alloy properties [16, 17]. By agreement with a consumer, the number of impurities under control (each with its separate upper specification limit) can be increased [14], but for simplicity, this is not discussed further in the current work.

Besides specification limits for the actual contents of the components, a narrower acceptance interval can be applied to test results with the purpose of decreasing the consumer's risks due to measurement uncertainty. In such a case, the decision rules (allowing to determine whether the alloy is conforming or not) are based on comparing test results with the acceptance limits [7, 18]. The acceptance limits in the present study are taken as coincidental with the specification limits.

2.2. Multivariate sub-domain of feasible alloy compositions

The specification limits of contents of the components, T_{Li} and T_{Ui}, form a multivariate specification domain of permissible alloy compositions. However, there are also two constraints of the mass balance to be satisfied: 1) sum of the contents of the base components and the eight impurities should be equal to 100 %, i.e. $c_1 + c_2 + c_4 = 100\ \%$, and 2) the content of the three precious impurities cannot exceed the content of the eight precious and non-precious impurities in the same alloy, i.e. $c_3 \leq c_4$. These constraints lead to a multivariate sub-domain of feasible alloy compositions. For example, at the Rh content $c_2 = T_{U2} = 7.7\ \%$ and the content of the eight

impurities $c_4 = T_{U4} = 0.18$ %, the Pt content is $c_1 = 92.12$ %, which is less than $T_{L1} = 92.2$ %, hence not permissible. On the other hand, such compositions as $c_1 = T_{L1}$, $c_2 = T_{U2}$, $c_3 \leq c_4$ and $c_4 = T_{U4}$ are within the specification domain, but cannot be realized in practice.

Therefore, in spite of the limitation $c_1 + c_2 + c_4 = 100$ %, typical for compositional data "consisting of vectors of positive components subject to a unit-sum constraint" [19], the multivariate sub-domain of feasible alloy compositions is more complex than a simplex of compositional data [20]. This sub-domain, having four dimensions, can be imagined as a kind of the three-dimensional simplex of c_1, c_2 and c_4, truncated by T_{Li} and T_{Ui} (i = 1, 2 and 4), while c_3 is the fourth dimension, limited by T_{U3} and influencing c_4 in the simplex, shown schematically in Fig.1.

Fig. 1

2.3. Test methods

Platinum ingots, rhodium powder and PtRh alloy wastes are melted in a vacuum induction furnace, providing homogeneity of the alloy. The melt is cast into graphite molds. Samples are cut down from an alloy ingot as a strip for preparation of two disks for wavelength dispersive X-ray fluorescence (XRF) analysis with an Axios spectrometer [21], measuring the Rh content. Samples in form of a band from the same ingot are prepared for optical atomic emission spectrometry (AES) analysis with a Baird spectrometer [22] for measurement of contents of the impurities. Metrologically traceable in-house reference materials are used for calibration of the spectrometers. Corresponding certified reference materials are described in the catalog [23].

A test result of the Pt content is calculated as a difference between 100 % and the test results of the Rh content and the content of the eight impurities according to the standard [24]: $c_{1m} = 100\ \% - c_{2m} - c_{4m}$.

3. Modelling and calculation

3.1. Analysis of raw data

3.1.1. Measurement uncertainty

The measurement procedures are validated according to the standard [25]. It was shown, based on the validation data, that (repeated) measurement results of the actual component contents [c_1, c_2, c_3, c_4] in the same sample have normal distributions. No interference of the analytes, which could be interpreted as a cause of correlation of test results and taken into account at the measurement uncertainty evaluation, was observed.

The validation reports include a value Δ (absolute measurement error' by ref. [26]) which is the expanded uncertainty of a measurement result with coverage factor 1.96 representing 95 % of a normal distribution: $\Delta = 1.96\sqrt{s_p^2 + s_t^2}$, where s_p is the intermediate precision standard deviation, and s_t is the standard uncertainty arising from the trueness estimation [27, 28], expressed in %. The corresponding standard measurement uncertainty is $u = \Delta/1.96$. For example, for a measured Rh content c_{2m} in the specification interval (7.3 – 7.7) %, Δ = 0.08 % and u_2 = 0.04 %.

Evaluation of the standard uncertainty u for an impurity is more complicated as Δ depends on the impurity content. In the report on validation of the optical AES procedure, the measuring interval of mass fractions [6] is divided into a number of sub-intervals in which Δ is considered constant. As an example, the u values corresponding to the mean values of the impurities' mass fractions observed in the 100 tested alloy batches are presented in Table 1. Standard uncertainty of measured content of the three precious impurities is $u_3 = \sqrt{u_{Pd}^2 + u_{Ir}^2 + u_{Au}^2}$ = 0.008 %. For measured content of the eight impurities, it is practically the same value $u_4 = \sqrt{u_{Fe}^2 + u_{Pb}^2 + u_{Si}^2 + u_{Sn}^2 + u_{Zn}^2 + u_{Pd}^2 + u_{Ir}^2 + u_{Au}^2}$ = 0.008 % (after rounding), since the Pd contribution u_{Pd} is dominant in both u_3 and u_4 budgets, as can be seen from Table 1. Standard uncertainty of the Pt content for this example is $u_1 = \sqrt{u_2^2 + u_4^2}$ = 0.041 %, when the content of the eight impurities in the alloy is as in Table 1, and the Rh content is in the specification interval.

For the calculations in the present work, a single value of the *relative* standard uncertainty of each impurity is considered on its whole measuring interval, rather than using sub-intervals, each with a constant standard uncertainty. For example, 18 such sub-intervals are in the validation report for mass fractions of Pd, Fe, Sn and Zn on the measuring interval from 0.0003 to 0.16 %.

Regression analysis of the dependence of the standard uncertainty on the element mass fraction w in middle of each sub-interval gives $u = 0.18\,w$ with coefficient of determination [29] $R^2 = 0.993$, corresponding to relative standard uncertainty $u_{rel} = 0.18$. For Ir, Pb, Au and Si the u_{rel} values are from 0.11 to 0.24.

The problem of using a single value of u_{rel} is that a given sum of the mass fractions of the impurities might consist of different combinations of the sum members. Each combination of the mass fractions of impurities is characterized by its associated measurement uncertainty, therefore the measurement uncertainty of the sum is ambiguous. However, because u_{Pd} is the dominant contribution in both u_3 and u_4, as shown above, for any measured value of content of the three and eight impurities c_{3m} and c_{4m}, respectively, the standard uncertainties $u_3 = 0.18\,c_{3m}$ and $u_4 = 0.18\,c_{4m}$ are used in the following calculations.

Then, the standard uncertainty of a measured Pt content c_{1m} is

$$u_1 = \sqrt{u_2^2 + u_4^2} = \sqrt{0.04^2 + (0.18\,c_{4m})^2}\,. \qquad (1)$$

3.1.2. Distributions of the test results

Histograms of the test results c_{im} are shown in Fig. 2 for: a) Pt, $i = 1$; b) Rh, $i = 2$; c) the three impurities, $i = 3$; and d) the eight impurities, $i = 4$. The mean m_i and standard deviation s_i of the test results are presented in Table 2.

Fig. 2

The s_i values are greater than measurement uncertainty u_i by about 1.5 times, since the batch-to-batch variation of test results is due to both the measurement uncertainty and the variation of the production/technological factors.

Table 2

Goodness-of-fit of theoretical normal distributions with unknown parameters to the empirical distributions of the data was tested by the Kolmogorov-Smirnov criterion [30]. The maximum absolute difference D_i between empirical and theoretical cumulative distribution functions, calculated using R software [31], are shown in Table 2. The critical values of D_i at $N = 100$ test results are $D_{crit} = 0.089$ for the level of confidence $P = 0.95$, and 0.103 for $P = 0.99$ [32]. When $D_i > D_{crit}$, then the null hypothesis that the distribution is normal at the chosen level of confidence P should be rejected. One can see from Table 2 that $D_3 > D_{crit}$ for the sum of the three impurities and $P = 0.95$. However, there is no D_i value exceeding D_{crit} for $P = 0.99$. Therefore, the null

hypothesis is not rejected at $P = 0.99$ for all tested alloy components. Corresponding theoretical normal probability density functions (pdfs) are shown in Fig. 2.

3.1.3. Correlation

Linear correlations among the test results for different components were estimated by Pearson's correlation coefficients r_{ij}, $i \neq j = 1, 2, 3, 4$, and reported in Table 3. The one-tailed critical values of the coefficient r_{crit} (when the correlation sign is known) for $N - 2 = 98$ degrees of freedom are 0.197 for level of confidence $P = 0.95$, and 0.256 for $P = 0.99$ [33, 34].

Test results for Rh are slightly correlated with mass fractions of impurities (statistically significant at $P = 0.95$ but insignificant at $P = 0.99$). This is possible as some part of the impurities came into the alloy with rhodium: the standard [35] permits up to 0.10 – 0.20 % of the impurities in different marks of Rh powder. Contents of the three and the eight impurities, limited by the constraint $c_3 \leq c_4$, have the correlation coefficient close to 1, as the content of the three impurities, especially of Pd, is the main contribution to the content of the eight impurities.

The contents of the base components of the alloy, Pt and Rh, have a high negative correlation: the greater the Rh content, the smaller is the Pt content. This is mainly due to the constraint on the mass fractions summing up to 100 %. Such correlation, specific for compositional data, is termed 'spurious' [36-38]. Also the correlations of the Pt content with the impurities' contents are negative for the same reason. Corresponding coefficients are significant at both levels of confidence, in spite of the fact that the impurities' contents in different marks of Pt ingots, used as a raw material, may be up to 0.07 – 0.20 % [14]. As in the case of Rh content vs. contents of the impurities, this is the reason for positive correlation.

Note, the correlation coefficients estimated analytically from the constraint $c_1 + c_2 + c_4 = 100$ % are for Pt vs. Rh contents $(r_{12})_{an} = -s_2/\sqrt{s_2^2 + s_4^2} = -0.961$, and for Pt vs. eight impurities' contents $(r_{14})_{an} = -s_4/\sqrt{s_2^2 + s_4^2} = -0.276$ (the standard deviations s_i are available in Table 2). The absolute values of $(r_{12})_{an}$ and $(r_{14})_{an}$ are even smaller than those of r_{12} and r_{14}, respectively, calculated directly from the experimental data, reported in Table 3. Thus, the observed correlations are caused as by the natural chemical origin of the raw materials used in the alloy production, as by the mass balance constraints, discussed in Section 2.2.

Taking into account the strong correlation between contents of the three and the eight impurities, as well as between contents of Rh and Pt, it is worthwhile to analyze the following two scenarios: 1) when measurement uncertainties of test results for all four components (i = 1 to 4) influence the probabilities of false decisions on the alloy conformity, and 2) when only two practically uncorrelated components - Rh and the eight impurities (i = 2 and 4) - are considered in this context, similar to 'principal components' [39-41]. Note also that there is no reason for 'spurious' correlation in the second scenario.

3.2. Modelling joint pdfs

There is an extensive literature stressing how traditional statistical techniques (such as moment estimates performed on skewed data) may produce inadequate results if applied on raw compositional data without suitable transformation [42-44]. However, introducing a methodology for a proper treatment of compositional data requires an isometric log-ratio or other transformation of the original experimental data. There might be no easy way to transform relevant estimates (results) back to the original variable space for conformity assessment purposes. Moreover, effectiveness of this methodology for an alloy is doubtful, since the multivariate sub-domain of feasible alloy compositions is more complex than a simplex of compositional data (Section 2.2).

In the present study, the effect of the mass balance constraints is embedded within the experimental correlation matrix (Table 3). It reflects a mixture of spurious correlation and the correlation caused by the native chemical properties of the raw materials used. This matrix influences all subsequent multivariate results. The univariate normal assumptions were tested for each component in Section 3.1.2. These assumptions were not affected by the compositional character of a part of the data, and there was no need to transform them in order to reach normality. The Bayesian framework for conformity assessment [7], implemented in ref. [10-12] for multicomponent materials and objects, is also followed here for modelling and calculating the total specific and global risks of false decisions in the alloy conformity assessment.

However, it is important to point out again that for another dataset the normal assumptions may be not adequate. When influence of such components like c_3 (not a subject to the unit-sum

constraint) is minimal, a kind of compositional data analysis [45, 46] taking into account properties of a truncated simplex could be helpful.

3.2.1. Prior pdfs

Pdfs of the theoretical normal distributions with means $\mu_i = m_i$ and standard deviations $\sigma_i = s_i$, shown in Fig. 2, are used as pdfs approximating the distributions of the actual components' content values c_i in the batches. A multivariate normal distribution was considered as the joint prior pdf for vector of actual components' contents [c_1, c_2, c_3, c_4] having vector of mean values [m_1, m_2, m_3, m_4]. The prior covariance matrix is

$$S_{c(1)} = \begin{pmatrix} 0.0065 & -0.0057 & -0.0007 & -0.0008 \\ -0.0057 & 0.0054 & 0.0003 & 0.0004 \\ -0.0007 & 0.0003 & 0.0004 & 0.0004 \\ -0.0008 & 0.0004 & 0.0004 & 0.0004 \end{pmatrix},$$

where the diagonal elements are variances $\sigma_i^2 = s_i^2$, (s_i are in Table 2), and the off-diagonal elements are covariances $cov_{ij} = r_{ij} \cdot \sigma_i \cdot \sigma_j$, $i \neq j$ (r_{ij} are in Table 3). Both σ_i^2 and cov_{ij} are expressed in squared %.

When only two components - Rh and the eight impurities (i = 2, 4) - are taken into account, the prior covariance matrix is

$$S_{c(2)} = \begin{pmatrix} 0.0054 & 0.0004 \\ 0.0004 & 0.0004 \end{pmatrix}.$$

The subscript in parentheses k = 1, 2 of the matrix symbol $S_{c(k)}$ indicates the scenario number.

3.2.2. Likelihood

The test results $c_{i\mathrm{m}}$ in the certificates, obtained following the laboratory measurement procedures, have normal distributions and measurement uncertainties as discussed above. Therefore, the vector [$c_{1\mathrm{m}}$, $c_{2\mathrm{m}}$, $c_{3\mathrm{m}}$, $c_{4\mathrm{m}}$] is modelled by a multivariate normal likelihood having

mean equal to the vector of actual components' contents [c_1, c_2, c_3, c_4] and covariance matrix defined on the base of measurement uncertainties u_i and correlation coefficients r_{ij}.

For test results $c_{i\mathrm{m}}$ equal, for example, to the prior means μ_i,= m_i (Table 2), the likelihood covariance matrix is:

$$S_{c\mathrm{m}(1)} = \begin{pmatrix} 0.0017 & -0.0016 & -0.0002 & -0.0002 \\ -0.0016 & 0.0016 & 0.0001 & 0.0001 \\ -0.0002 & 0.0001 & 0.0001 & 0.0001 \\ -0.0002 & 0.0001 & 0.0001 & 0.0001 \end{pmatrix},$$

where the diagonal elements are variances $u_1^2 = 0.04^2 + (0.18\, c_{4\mathrm{m}})^2$ by eqn. (1), $u_2^2 = 0.04^2$, $u_3^2 = (0.18\, c_{3\mathrm{m}})^2$ and $u_4^2 = (0.18\, c_{4\mathrm{m}})^2$. The covariances are $cov_{ij\mathrm{m}} = r_{ij} \cdot u_i \cdot u_j$, $i \neq j$ (r_{ij} as in Table 3). Values u_i^2 and $cov_{ij\mathrm{m}}$ are expressed in squared %. The subscript in parentheses k of the matrix symbol $S_{c\mathrm{m}(k)}$ indicates the same number of the scenario as for $S_{c(k)}$ above.

For the scenario with Rh and the eight impurities only (i = 2 and 4), the likelihood covariance matrix, in the case when the test results $c_{i\mathrm{m}}$ are equal to prior means μ_i,= m_i (Table 2), is:

$$S_{c\mathrm{m}(2)} = \begin{pmatrix} 0.0016 & 0.0001 \\ 0.0001 & 0.0001 \end{pmatrix}.$$

Note that in a case when a consumer decides to test the alloy batches in its own laboratory, or in a contract certification laboratory, the measurement methods, instruments, staff – i.e. the uncertainty contributions – may be different from those in the plant laboratory. In such a case the likelihood may be different from a multivariate normal pdf and cannot rely on to the plant laboratory measurement uncertainties.

3.2.3. Posterior pdf

As the actual content values of the four components in the current study are jointly described by a multivariate prior normal pdf, and the likelihood of their test results is also modelled by a multivariate normal pdf, the joint posterior pdf is a multivariate normal pdf, as well. The posterior pdf has the following parameters [12, 47]:

$$S_{\mathrm{p}(k)} = (S_{\mathrm{c}(k)}^{-1} + n_{\mathrm{rep}}\, S_{\mathrm{cm}(k)}^{-1})^{-1} \text{ and } \boldsymbol{c}_{\mathrm{p}(k)} = S_{\mathrm{p}(k)}(S_{\mathrm{c}(k)}^{-1}\boldsymbol{c} + n_{\mathrm{rep}}\, S_{\mathrm{cm}(k)}^{-1}\, \overline{\boldsymbol{c}_{\mathrm{m}}})^{-1}, \quad (2)$$

where $S_{\mathrm{p}(k)}$ and $\boldsymbol{c}_{\mathrm{p}(k)}$ are the posterior covariance matrix and the vector of the posterior means, respectively; $\boldsymbol{c}$ is the vector of the prior mean values [μ_1, μ_2, μ_3, μ_4], where $\mu_i = m_i$; $\overline{\boldsymbol{c}_{\mathrm{m}}}$ is the vector of the arithmetic means of n_{rep} replicate measurement/test results (in this study, for a single test result, n_{rep} = 1 and $\overline{\boldsymbol{c}_{\mathrm{m}}} = \boldsymbol{c}_{\mathrm{m}} = [c_{1\mathrm{m}}, c_{2\mathrm{m}}, c_{3\mathrm{m}}, c_{4\mathrm{m}}]$). As an example, for the vector of measurement results $\boldsymbol{c}_{\mathrm{m}} = [92.423, 7.457, 0.120, 0.120]$, the posterior covariance matrix is

$$S_{\mathrm{p}(1)} = \begin{pmatrix} 7.6741 & -8.5547 & 0.6761 & 0.8088 \\ -8.5547 & 9.6566 & -0.9075 & -1.0709 \\ 0.6761 & -0.9075 & 0.4016 & 0.3144 \\ 0.8088 & -1.0709 & 0.3144 & 0.3510 \end{pmatrix} \times 10^{-4},$$

and the vector of the posterior means is $\boldsymbol{c}_{\mathrm{p}(1)}$ = [92.405, 7.481, 0.104, 0.111].

Under scenario k = 2 with two components only (i = 2 and 4), for the vector of measurement results $\boldsymbol{c}_{\mathrm{m}} = [7.457, 0.120]$ corresponding to the example above, the posterior covariance matrix is:

$$S_{\mathrm{p}(2)} = \begin{pmatrix} 0.0012 & 0.0001 \\ 0.0001 & 0.0002 \end{pmatrix},$$

and the vector of the posterior means is $\boldsymbol{c}_{\mathrm{p}(2)}$ = [7.452, 0.088].

3.3. Computational details

Calculation of parameters of the posterior multivariate normal distribution by eqn. (2) and descending specific risk values were performed in the R programming environment as described in ref. [12]. Simulation of the posterior distribution is also possible by Markov Chain Monte Carlo (MCMC), using the Metropolis-Hasting algorithm and Cholesky decomposition of the covariance matrix with MS Excel [48]. The analytical solution (2), for parameters of the posterior pdf and corresponding risk values, is more accurate by definition than the MCMC solution, even with a large number of trials. On the other hand, an analytical solution is not always available, especially when prior and likelihood pdfs are more complicated than normal

[12]. In the present study, analytical and simulated MCMC results (parameters of the posterior pdf and risk values) practically coincided.

Core of the R code, used for calculations in this paper, is presented in Appendix A.

4. Results and discussion

4.1. Specific risks

For any vector of measurement/test results [c_{1m}, c_{2m}, c_{3m}, c_{4m}] within the multivariate specification domain, the total specific consumer's risk R^*_{total} is calculated as one minus the integral of the posterior pdf on this domain. That is the probability of at least one of the actual components' content lying outside its own specification interval. R^*_{total} values are dependent on the measured *i*-th component content c_{im} as shown in Fig. 3 by line 1. The c_{im} values are on their specification intervals, i.e. from T_{Li} to T_{Ui}.

Fig. 3

The risk values plotted against the measured Pt content c_{1m} are in Fig. 3a. The sub-domain spreads from c_{1m} = 100 % – T_{U2} – c_{4m} = 92.24 % (line 2) to c_{1m} = 100 % – T_{L2} – c_{4m} = 92.64 % (line 3). That is because the Rh upper and lower specification limits are T_{U2} = 7.7 % and T_{L2} = 7.3 %, respectively, and the assumed content of eight impurities in this case is equal to its prior mean, c_{4m} = 0.059 %. The assumed content of the three impurities is also equal to its prior mean: c_{3m} = 0.052 %. Line 4 indicates the minimum observed value c_{1m}, whereas line 3 coincides with the maximum observed value.

The dependence of the total specific risk on the component content can be used for setting acceptance limits, and for quality control charts [49]. For example, c_{1m} = 92.25 and 92.59 %, at which R^*_{total} = 0.01 in Fig. 3a, may be applied as the warning lines in the alloy control chart, and c_{1m} = 92.61 % at which R^*_{total} = 0.05 as the action line.

Fig. 3b refers to Rh content c_{2m} at c_{1m} = 100 % – c_{2m} – c_{4m}, c_{3m} = 0.052 % and c_{4m} = 0.059 % as in Fig. 3a. Lines 2 and 3 show the minimum and maximum observed values of c_{2m}. R^*_{total} dependences on c_{1m} in Fig. 3a and on c_{2m} in Fig. 3b have a specular reflection behavior, since the fixed values of c_{3m} and c_{4m} are the same. Thus, c_{1m} and c_{2m} are the members of the same mass balance equation. The possible warning lines here are c_{2m} = 7.35 and 7.69 % (R^*_{total} = 0.01 in Fig. 3b). The candidate for the action line is c_{2m} = 7.33 % (R^*_{total} = 0.05).

Fig. 3c is for R^*_{total} against content $c_{3\mathrm{m}}$ of the three impurities at $c_{1\mathrm{m}}$ = 100 % – $c_{2\mathrm{m}}$ – $c_{4\mathrm{m}}$ and $c_{2\mathrm{m}}$ = 7.46 %. Taking into account the constraint $c_{3\mathrm{m}} \leq c_{4\mathrm{m}}$, the content of the eight impurities $c_{4\mathrm{m}}$ is set using the mean ratio between $c_{3\mathrm{m}}$ and $c_{4\mathrm{m}}$, according to which $c_{4\mathrm{m}}$ = 1.16 $c_{3\mathrm{m}}$. Lines 2 and 3 indicate the minimum and maximum $c_{3\mathrm{m}}$ values. The warning line is $c_{3\mathrm{m}}$ = 0.113 % (R^*_{total} = 0.01 in Fig. 3c) and the action line is $c_{3\mathrm{m}}$ = 0.117 % (R^*_{total} = 0.05).

Fig. 3d demonstrates the risk dependence on content $c_{4\mathrm{m}}$ of the eight impurities at $c_{1\mathrm{m}}$ = 100 % – c_{m2} – $c_{4\mathrm{m}}$, $c_{2\mathrm{m}}$ = 7.46 % and $c_{3\mathrm{m}}$ = $c_{4\mathrm{m}}$ /1.16. Since the upper specification limit for $c_{3\mathrm{m}}$ is T_{U3} = 0.12 %, $c_{3\mathrm{m}}$ was required to be below 0.12 % at any $c_{4\mathrm{m}}$ value. Lines 2 and 3 are again the minimum and maximum $c_{4\mathrm{m}}$ values. The warning line in Fig. 3d is $c_{4\mathrm{m}}$ = 0.131 % (R^*_{total} = 0.01) and the action line is $c_{3\mathrm{m}}$ = 0.137 % (R^*_{total} = 0.05). One can see in Fig. 3d that the observed $c_{4\mathrm{m}}$ values are sufficiently far from both the warning and action lines.

The values R^*_{total} vs. $c_{i\mathrm{m}}$ in Fig. 3 are examples calculated at particular values of $c_{j\mathrm{m}}$, $i \neq j$. More information can be provided using a three-dimensional representation, as in Fig. 4, where surfaces of R^*_{total} vs. $c_{2\mathrm{m}}$ and $c_{4\mathrm{m}}$ are shown. The plot in Fig. 4a is for the four-component scenario at $c_{3\mathrm{m}}$ = $c_{4\mathrm{m}}$ /1.16, but not exceeding 0.12 %, and 92.2 % ≤ $c_{1\mathrm{m}}$ = 100 % – $c_{2\mathrm{m}}$ – $c_{4\mathrm{m}}$ ≤ 92.8 %. The color column bar gives indication of the risk between minimum 0 and maximum 1 on the surface. The risk slightly increases with $c_{2\mathrm{m}}$ near both the specification limits of the Rh content and more significantly at $c_{4\mathrm{m}}$ approaching its upper specification limit. This behavior corresponds to the two-dimensional dependences in Fig. 3, discussed above.

Fig. 4

The plot in Fig. 4b shows the surface of the risks for the two-component scenario of the practically independent $c_{2\mathrm{m}}$ and $c_{4\mathrm{m}}$. Note that the maximum risk value for this scenario is only 0.26, in contrast to nearly 1 when all four components are considered. One can see that simplification of the conformity assessment task from four- to two-component scenario leads to undervaluation of R^*_{total}: its maximum value in Fig. 4b is four times smaller than in Fig. 4a. The form of the surfaces is also different. In particular, the surface in Fig. 4b is less sensitive to $c_{4\mathrm{m}}$ increasing in comparison to the four-component scenario in Fig. 4a. In other words, the simplification is not usable, since the observed strong correlation increases significantly and complicates the dependence of specific risks R^*_{total} on the test results.

4.2. Global risks

The total global consumer's risk R_{total} is calculated, as in the study [12], on the base of integrals [50] of the product of the prior and likelihood pdfs. The obtained small value of $R_{\text{total}} = 5.6\times10^{-7}$ is an indication of a reliable quality assurance system.

To understand the influence of correlation on R_{total}, the risk was estimated for a simulated case of uncorrelated contents of the components [10, 51]. This simulation was carried out by setting all correlation coefficients $r_{ij} = 0$ ($i \neq j$), hence transforming $S_{c(k)}$ and $S_{\text{cm}(k)}$ into diagonal matrices. The result $R_{\text{total}} = 6.2\times10^{-3}$ was four orders of magnitude greater than for the correlated contents. In fact, the strong correlation between c_1 and c_2 and between c_3 and c_4 ties the variables together, dramatically decreasing the risk whenever all the measured quantities are within their acceptance intervals, while at least one of the actual components' content values is outside its specification interval. Thus, the total global consumer's risk for strongly correlated contents of the components is much smaller than for uncorrelated contents, a fact observed also in ref. [12].

In the framework of the scenario $k = 2$, when c_2 and c_4 only are taken into account, the risk is $R_{\text{total}} = 5.1\times10^{-3}$ for correlated contents, and $R_{\text{total}} = 4.9\times10^{-3}$ for contents simulated as uncorrelated. It is seen that the risk is not practically affected by the observed (small) correlation between these two components' contents. The risk for two simulated uncorrelated contents (4.9×10^{-3}) is a little smaller than that for four uncorrelated ones (6.2×10^{-3}), as predicted in ref. [10]. Both these values, and also the risk for the scenario of two correlated contents (5.1×10^{-3}) are of the same order of magnitude. Therefore, reducing the number of components under control would lead to practically the same overestimation of the global risk as neglecting the strong correlation among the four components contents.

Note, the total global consumer's risk $R_{\text{total}} = 5.1\times10^{-3}$ for the case of control of Rh content and content of the eight impurities (scenario $k = 2$) means accepting one non-compliant alloy batch in 200 produced batches, when it should have been rejected. Since 100 batches were produced during about two years at the plant, this false decision would be expected on average once every four years assuming unchanged conditions. However, *de-facto* each batch is tested according to the standards [14] and [22] for contents of the four components (scenario $k = 1$). The greater amount of information, available in this case, decreases the risk of false decisions in spite of the complexity of the correlations among the test results. The risk value $R_{\text{total}} = 5.6\times10^{-7}$

means that there is no practical chance for a non-compliant alloy batch to find a way out of the plant to the market.

The counterpart models for the total producer's risks are easily obtainable.

5. Conclusions

Total risk (probability) of a false decision on conformity of an alloy due to measurement uncertainty and correlation of test results is quantified. As an example, a dataset of test results of a PtRh alloy is studied when four components of its composition are under control. Since correlations among test results for two pairs of the components were strong, the study was performed for two scenarios: considering contents of all the four components in the first scenario, and only two practically independent components' contents – in the second.

A matrix Bayesian approach is applied for total risk evaluation, where the observed correlations caused by the natural chemical origin of the raw materials used in the alloy production, and by the mass balance constraints, are taken into account within the experimental correlation matrix. This matrix influenced all subsequent multivariate calculation results.

The dependence of total specific risk (for a specified alloy batch) on the alloy test results was calculated and demonstrated using two- and three-dimensional plots. Total global risk (for a batch randomly drawn from a statistical population of such batches) was calculated as being very small, which is an indication of a reliable quality assurance system of the manufacture of alloys. Comparing the two scenarios, it was shown that taking into account all four correlated contents of the components, as is the current practice, decreases the global risk significantly with respect to the simulated simplifications.

The R code presented here, used for risk calculations, may be helpful in similar investigations.

Acknowledgements

The authors would like to express their gratitude to the Central Laboratory of the JSC Ekaterinburg Non-Ferrous Metal Processing Plant (EZOCM), Russia, for providing the raw data on the PtRh alloy used in the present study.

This research was supported in part by the International Union of Pure and Applied Chemistry (IUPAC Project 2016-007-1-500).

Appendix A. Core of the R code

A.1. Calculation of the total specific consumer's risk

```
# Initializations and settings
lsl1 = 92.2             # Lower specification limit
usl1 = 92.8             # Upper specification limit
lsl2 = 7.3              # Lower specification limit
usl2 = 7.7              # Upper specification limit
lsl3 = 0                # Lower specification limit
usl3 = 0.12             # Upper specification limit
lsl4 = 0                # Lower specification limit
usl4 = 0.18             # Upper specification limit

mu1 = 92.483            # Prior mean value
mu2 = 7.457             # Prior mean value
mu3 = 0.052             # Prior mean value
mu4 = 0.059             # Prior mean value
uc1 = 0.081             # Prior uncertainty
uc2 = 0.073             # Prior uncertainty
uc3 = 0.019             # Prior uncertainty
uc4 = 0.021             # Prior uncertainty
ucm1 = sqrt(0.04^2+0.18^2*mu4^2)/mu1*100      # Relative (%) measurement uncertainty
ucm2 = 0.04/mu2*100                           # Relative (%) measurement uncertainty
ucm3 = 0.18*100                               # Relative (%) measurement uncertainty
ucm4 = 0.18*100                               # Relative (%) measurement uncertainty

# Prior covariance matrix
Sc = diag(4)
Sc[1,1] = uc1^2
Sc[2,2] = uc2^2
Sc[3,3] = uc3^2
Sc[4,4] = uc4^2
Sc[2,1] = Sc[1,2] <-  -0.967*uc1*uc2
Sc[3,1] = Sc[1,3] <-  -0.469*uc1*uc3
```

```
Sc[4,1] = Sc[1,4] <-  -0.467*uc1*uc4
Sc[3,2] = Sc[2,3] <-   0.239*uc2*uc3
Sc[4,2] = Sc[2,4] <-   0.228*uc2*uc4
Sc[4,3] = Sc[3,4] <-   0.970*uc3*uc4
Sc

# Likelihood covariance matrix
# NOTE: each term in Scm is to be multiplied by cim*cjm in order to get the covariance matrix
Scm = diag(4)
Scm[1,1] = ucm1^2
Scm[2,2] = ucm2^2
Scm[3,3] = ucm3^2
Scm[4,4] = ucm4^2
Scm[2,1] = Scm[1,2] <- -0.967*ucm1*ucm2
Scm[3,1] = Scm[1,3] <- -0.469*ucm1*ucm3
Scm[4,1] = Scm[1,4] <- -0.467*ucm1*ucm4
Scm[3,2] = Scm[2,3] <-  0.239*ucm2*ucm3
Scm[4,2] = Scm[2,4] <-  0.228*ucm2*ucm4
Scm[4,3] = Scm[3,4] <-  0.970*ucm3*ucm4
Scm

################
# SR1: total specific risk for the FIRST component
library(mvtnorm)
step = 0.001                          # Increasing step for the measured values
lower = c(lsl1,lsl2,lsl3,lsl4)        # Lower specification limits
upper = c(usl1,usl2,usl3,usl4)        # Upper specification limits
n=1                                   # Number of repeated measurements for the component
Scinv = solve(Sc)                     # Inverse matrix of Sc
c3m = mu3                             # Fixed considered value for c3m
c4m = mu4                             # Fixed considered value for c4m
t1 = seq(100 - c4m - usl2,100 - c4m - lsl2,step)      # Values which the component can get
SR1 = rep(0,length(t1))                               # Initialization of the vector of the risk
# values

for (i in 1:length(t1))
{
        c1m = t1[i]
        c2m = 100 - c4m - c1m                 # Constraint on c2m
        Scminv = solve(t(c(c1m,c2m,c3m,c4m)*Scm/10000)*c(c1m,c2m,c3m,c4m))
        varPost = solve(Scinv  + n*Scminv)
        muPost = crossprod(varPost, (crossprod(Scinv,c(mu1,mu2,mu3,mu4)) +
crossprod(n*Scminv,c(mean(c1m),mean(c2m),mean(c3m),mean(c4m)))) )
        muP = as.vector(muPost)
        SR1[i] = 1 - pmvnorm(lower, upper, mean = muP, sigma = varPost)
}
```

```
SR1                                  # Vector of the total specific risk values for the component
```

Notes:

1. Use of relative measurement uncertainties of Rh content as ucm2 = 0.04/mu2*100, and of Pt content as ucm1 = sqrt(0.04^2+0.18^2*mu4^2)/mu1*100, is an approximation in the code, acceptable because of the narrow specification intervals for Pt and Rh.

2. Time spent for calculation with an ordinal PC is less than two seconds when step = 0.001, and less than eight seconds when step = 0.0001.

A.2. Calculation of the total global consumer's risk

Consider the same "Initializations and settings" and the same covariance matrices as in calculation of the total specific consumer's risk.

```
# Multivariate normal prior pdf: [c1, c2, c3, c4] ~ MVN(c(mu1,mu2,mu3,mu4),Sc)
# where Sc is the 4 x 4 covariance prior matrix
# Multivariate normal likelihood: [c1m,c2m,c3m,c4m|c1,c2,c3,c4] ~
# MVN(c(c1,c2,c3,c4),Scm_mod)
# where Scm_mod = t(c(c1m,c2m,c3m,c4m)*Scm/10000)*c(c1m,c2m,c3m,c4m) and
# Scm is the 4 x 4 likelihood covariance matrix above defined.
# The consumer global risk GRc is made by the sum of several terms, each being a multiple
# integral of the prior pdf times the likelihood, where dummy variables x[1-4] of the prior pdf
# vary outside the specification domain, whereas the measured values x[5-8] of the likehood
# vary inside the acceptance domain (equivalent to the specification domain, here).

# For 4 components
library(cubature)
# Defintion of the function to be integrated: product of the prior pdf and the likelihood
Jointpdf = function(x)  {dmvnorm(c(x[1],x[2],x[3],x[4]), mean = c(mu1,mu2,mu3,mu4), sigma =
Sc)  *  dmvnorm(c(x[5],x[6],x[7],x[8]),  mean  =  c(x[1],x[2],x[3],x[4]),  sigma  =
t(c(x[5],x[6],x[7],x[8])*Scm/10000)*c(x[5],x[6],x[7],x[8])) }

ME = 10^6                            # Maximum number of function evaluations

CB1A  =  adaptIntegrate(Jointpdf,  lowerLimit  =  c(92,7,0,0,lower),  upperLimit  =
c(92.2,8,0.13,0.19, upper), maxEval = ME)
CB1B  =  adaptIntegrate(Jointpdf,  lowerLimit  =  c(92.8,7,0,0,lower),  upperLimit  =
c(93,8,0.13,0.19, upper), maxEval = ME)
CB1 = CB1A$integral + CB1B$integral
CB1  #  4.163485e-24 (ME=10^5); 4.156291e-24 (ME=10^6)
```

```
CB2A = adaptIntegrate(Jointpdf, lowerLimit = c(92,7,0,0,lower), upperLimit = c(93,7.3,0.13,0.19, upper), maxEval = ME)
CB2B = adaptIntegrate(Jointpdf, lowerLimit = c(92,7.7,0,0,lower), upperLimit = c(93,8,0.13,0.19, upper), maxEval = ME)
CB2 = CB2A$integral + CB2B$integral
CB2 #  3.191624e-07 (ME=10^5); 5.599096e-07 (ME=10^6)

CB3B = adaptIntegrate(Jointpdf, lowerLimit = c(92,7,0.12,0,lower), upperLimit = c(93,8,0.13,0.19, upper), maxEval = ME)
CB3 = CB3B$integral
CB3 # 4.221176e-11 (ME=10^5); 2.779241e-11 (ME=10^6)

CB4B = adaptIntegrate(Jointpdf, lowerLimit = c(92,7,0,0.18,lower), upperLimit = c(93,8,0.13,0.19, upper), maxEval = ME)
CB4 = CB4B$integral
CB4 # 0 (ME=10^5); 0 (ME=10^6)

CB1B2A = adaptIntegrate(Jointpdf, lowerLimit = c(92,7,0,0,lower), upperLimit = c(92.2,7.3,0.13,0.19, upper), maxEval = ME)
CB1B2B = adaptIntegrate(Jointpdf, lowerLimit = c(92.8,7.7,0,0,lower), upperLimit = c(93,8,0.13,0.19, upper), maxEval = ME)
CB1B2 = CB1B2A$integral + CB1B2B$integral
CB1B2 # 0 (ME=10^6); 0 (ME=10^6)

CB1B3A = adaptIntegrate(Jointpdf, lowerLimit = c(92,7,0.12,0,lower), upperLimit = c(92.2,8,0.13,0.19, upper), maxEval = ME)
CB1B3B = adaptIntegrate(Jointpdf, lowerLimit = c(92.8,7,0.12,0,lower), upperLimit = c(93,8,0.13,0.19, upper), maxEval = ME)
CB1B3 = CB1B3A$integral + CB1B3B$integral
CB1B3 # 3.155852e-69 (ME=10^5); 3.359202e-69 (ME=10^6)

CB1B4A = adaptIntegrate(Jointpdf, lowerLimit = c(92,7,0,0.18,lower), upperLimit = c(92.2,8,0.13,0.19, upper), maxEval = ME)
CB1B4B = adaptIntegrate(Jointpdf, lowerLimit = c(92.8,7,0,0.18,lower), upperLimit = c(93,8,0.13,0.19, upper), maxEval = ME)
CB1B4 = CB1B4A$integral + CB1B4B$integral
CB1B4 # 0 (ME=10^5); 0 (ME=10^6)

CB2B3A = adaptIntegrate(Jointpdf, lowerLimit = c(92,7,0.12,0,lower), upperLimit = c(93,7.3,0.13,0.19, upper), maxEval = ME)
CB2B3B = adaptIntegrate(Jointpdf, lowerLimit = c(92,7.7,0.12,0,lower), upperLimit = c(93,8,0.13,0.19, upper), maxEval = ME)
CB2B3 = CB2B3A$integral + CB2B3B$integral
CB2B3 # 2.9111e-21 (ME=10^5); 6.390908e-20 (ME=10^6)
```

```
CB2B4A = adaptIntegrate(Jointpdf, lowerLimit = c(92,7,0,0.18,lower), upperLimit = c(93,7.3,0.13,0.19, upper), maxEval = ME)
CB2B4B = adaptIntegrate(Jointpdf, lowerLimit = c(92,7.7,0,0.18,lower), upperLimit = c(93,8,0.13,0.19, upper), maxEval = ME)
CB2B4 = CB2B4A$integral + CB2B4B$integral
CB2B4 # 0 (ME=10^5); 0 (ME=10^6)

CB3B4A = adaptIntegrate(Jointpdf, lowerLimit = c(92,7,0.12,0.18,lower), upperLimit = c(92,8,0.13,0.19, upper), maxEval = ME)
CB3B4 = CB3B4A$integral
CB3B4 # 0 (ME=10^5); 0 (ME=10^6)

CB1B2B3A = adaptIntegrate(Jointpdf, lowerLimit = c(92,7,0.12,0,lower), upperLimit = c(92.2,7.3,0.13,0.19, upper), maxEval = ME)
CB1B2B3B = adaptIntegrate(Jointpdf, lowerLimit = c(92.8,7.7,0.12,0,lower), upperLimit = c(93,8,0.13,0.19, upper), maxEval = ME)
CB1B2B3 = CB1B2B3A$integral + CB1B2B3B$integral
CB1B2B3 # 0 (ME=10^5); 0 (ME=10^6)

CB1B2B4A = adaptIntegrate(Jointpdf, lowerLimit = c(92,7,0,0.18,lower), upperLimit = c(92.2,7.3,0.13,0.19, upper), maxEval = ME)
CB1B2B4B = adaptIntegrate(Jointpdf, lowerLimit = c(92.8,7.7,0,0.18,lower), upperLimit = c(93,8,0.13,0.19, upper), maxEval = ME)
CB1B2B4 = CB1B2B4A$integral + CB1B2B4B$integral
CB1B2B4 # 0 (ME=10^5); 0 (ME=10^6)

CB1B3B4A = adaptIntegrate(Jointpdf, lowerLimit = c(92,7,0.12,0.18,lower), upperLimit = c(92.2,8,0.13,0.19, upper), maxEval = ME)
CB1B3B4B = adaptIntegrate(Jointpdf, lowerLimit = c(92.8,7,0.12,0.18,lower), upperLimit = c(93,8,0.13,0.19, upper), maxEval = ME)
CB1B3B4 = CB1B3B4A$integral + CB1B3B4B$integral
CB1B3B4 # 0 (ME=10^5); 0 (ME=10^6)

CB2B3B4A = adaptIntegrate(Jointpdf, lowerLimit = c(92,7,0.12,0.18,lower), upperLimit = c(93,7.3,0.13,0.19, upper), maxEval = ME)
CB2B3B4B = adaptIntegrate(Jointpdf, lowerLimit = c(92,7.7,0.12,0.18,lower), upperLimit = c(93,8,0.13,0.19, upper), maxEval = ME)
CB2B3B4 = CB2B3B4A$integral + CB2B3B4B$integral
CB2B3B4 # 0 (ME=10^5); 0 (ME=10^6)

CB1B2B3B4A = adaptIntegrate(Jointpdf, lowerLimit = c(92,7,0.12,0.18,lower), upperLimit = c(92.2,7.3,0.13,0.19, upper), maxEval = ME)
CB1B2B3B4B = adaptIntegrate(Jointpdf, lowerLimit = c(92.8,7.7,0.12,0.18,lower), upperLimit = c(93,8,0.13,0.19, upper), maxEval = ME)
CB1B2B3B4 = CB1B2B3B4A$integral + CB1B2B3B4B$integral
CB1B2B3B4  # 0 (ME=10^5); 0 (ME=10^6)
```

```
# Formula for the total global risk
GRc = CB1 + CB2 + CB3 + CB4 - CB1B2 - CB1B3 - CB1B4 - CB2B3 - CB2B4 - CB3B4 +
CB1B2B3 + CB1B2B4 + CB1B3B4 + CB2B3B4 - CB1B2B3B4
GRc  # 3.192046e-07 (ME = 10^5); 5.599374e-07 (ME = 10^6)
```

Notes:

1. The integration intervals for integrating out dummy variables x[1-4] (actual content values of the components) were chosen encompassing the bulk of the distributions shown in Fig. 2: [92, 93], [7, 8], [0, 0.13] and [0, 0.19] for x[1], x[2], x[3] and x[4], respectively.

2. Time spent for calculation with an ordinal PC is less than two minutes when ME = 10^5, and about 23 minutes when ME = 10^6.

3. Validation of the code in the case of four uncorrelated variables with respect to analytical expressions in ref. [10, 11] showed a relative error of about 29 % when using ME = 10^6 (GRc = 0.0062 to be compared with the analytical solution equal to 0.0048). For the scenario for two variables the relative error is about 4 % (GRc = 0.0049 to be compared with the analytical solution equal to 0.0047). They are acceptable errors taking into account the order of magnitude of the compared risk values.

References

[1] T. Cvitaš, Quantities describing compositions of mixtures, Metrologia 33 (1996) 35-39.

[2] X. Fuentes-Arderiu, Concentration and content, Biochemia Medica 23/2 (2013) 141-142.

[3] T.J. Tolhurst, A.J. Underwood, R.G. Perkins, M.G. Chapman, Content versus concentration: Effects of units on measuring the biogeochemical properties of soft sediments, Estuarine, Coastal and Shelf Science 63 (2005) 665-673.

[4] M. Dobbert, Setting and using specifications – An overview, Measure 5/3 (2010) 68-73.

[5] J.L. Smith, The role of specification limits, Quality Magazine (2017) 1-3. <https://www.qualitymag.com/articles/94158-the-role-of-specification-limits> (Accessed July 2018).

[6] Joint Committee for Guides in Metrology, JCGM 200:2012, International Vocabulary of

Metrology – Basic and General Concepts and Associated Terms. <http://www.bipm.org/en/publications/guides/vim.html> (Accessed May 2018).

[7] Joint Committee for Guides in Metrology, JCGM 106:2012, Evaluation of Measurement Data – The Role of Measurement Uncertainty in Conformity Assessment. <http://www.bipm.org/utils/common/documents/jcgm/JCGM_106_2012_E.pdf> (Accessed May 2018).

[8] European Commission, Grows Internal Market, Industry, Entrepreneurship and SMEs. <https://ec.europa.eu/growth/single-market/goods/building-blocks/conformity-assessment_en> (Accessed May 2018).

[9] IUPAC Project 2016-007-1-500, Risk of conformity assessment of multicomponent material or object in relation to measurement uncertainty of its test results. <http://iupac.org/project/2016-007-1-500> (Accessed May 2018).

[10] I. Kuselman, F.R. Pennecchi, R.J.N.B. da Silva, D.B. Hibbert, Conformity assessment of multicomponent materials or objects: Risk of false decisions due to measurement uncertainty – A case study of denatured alcohols, Talanta 164 (2017)189-195.

[11] F.R. Pennecchi, I. Kuselman, R.J.N.B. da Silva, D.B. Hibbert, Risk of false decision on conformity of an environmental compartment due to measurement uncertainty of concentrations of two or more pollutants, Chemosphere 202 (2018) 165-176.

[12] I. Kuselman, F.R. Pennecchi, R.J.N.B. da Silva, D.B. Hibbert, Risk of false decision on conformity of a multicomponent material when test results of the components' content are correlated, Talanta 174 (2017) 789-796.

[13] American Elements. Platinum Rhodium Alloy. <https://www.americanelements.com/platinum-rhodium-alloy-11107-71-4> (Accessed May 2018).

[14] GOST 13498:2010, Platinum and its base alloys. Marks, Standardinform, Moscow.

[15] Ekaterinburg Non-Ferrous Metal Processing Plant. <http://www.ezocm.ru/en/> (Accessed May 2018).

[16] B. Trumić, L. Gomidželović, S. Marjanović, A. Ivanović, V. Krstić, Platinum-based alloys: investigation of the effect of impurities content on creep rate, rupture time and relative elongation at high temperatures, Mat Res 20/1 (2017). <http://dx.doi.org/10.1590/1980-5373-mr-2016-0240> (Accessed May 2018).

[17] V. Ponec, Alloy catalysts: the concepts, Appl Catal A, General 222 (2001) 31-45.

[18] S.L.R. Ellison and A. Williams, (Eds), EURACHEM/CITAC Guide: Use of Uncertainty Information in Compliance Assessment, 2007. <www.eurachem.org> (Accessed May 2018).

[19] J. Aitchison, The Statistical Analysis of Compositional Data, Chapman & Hall, London, 1986.

[20] J. Aitchison, Principles of compositional data analysis. In: T.W. Anderson, K.T. Fang and I. Olkin, (Eds), Multivariate Analysis and its Applications, IMS Lecture Notes – Monograph Series, Hayward, CA: Institute of Mathematical Statistics, Vol. 24, 1994, pp. 73-81, DOI:10.1214/lnms/1215463786.

[21] PANanalytial, Model Axious XRF-Spectrometers. <https://www.environmental-expert.com/products/model-axios-xrf-spectrometers-19076> (Accessed May 2018).

[22] HighBeam Research, Baird Corporation. <https://www.highbeam.com/doc/1G1-16138028.html> (Accessed May 2018).

[23] Ekaterinburg Non-Ferrous Metal Processing Plant, Certified reference materials. <http://www.ezocm.ru/en/catalog/certified_reference_materials/platinum_and_platinum_alloys/> (Accessed May 2018).

[24] GOST R 52599:2006, Precious metals and their alloys, General requirements for methods of analysis, Standardinform, Moscow.

[25] GOST R 8.563:2009, State system for ensuring the uniformity of measurements. Procedures of measurements, Standardinform, Moscow.

[26] Recommendation MI 1317:2004, State system for ensuring the uniformity of measurements. Results and characteristics of measurement errors. Forms of representation. Methods of use for testing samples of a product and control of their parameters, All-Russian Research Institute of Metrological Service (VNIIMS), Moscow.

[27] ISO 21748:2017, Guidance for the use of repeatability, reproducibility and trueness estimates in measurement uncertainty evaluation, 2nd edn., ISO, Geneva.

[28] S.L.R.Ellison and A. Williams, (Eds), Eurachem/CITAC Guide: Quantifying uncertainty in analytical measurement, 3rd edn., 2012. <https://www.eurachem.org/index.php/publications/guides> (Accessed May 2018).

[29] D. Ozer, Correlation and coefficient of determination. Psychological Bulletin 97 (1985) 307- 315, DOI: 10.1037/0033-2909.97.2.307.

[30] P.J. Kim and R.I. Jennrich, Tables of the exact sampling distribution of the two-sample Kolmogorov-Smirnov criterion. In: H.L. Harter and D.B. Owen, (Eds), Selected Tables in Mathematical Statistics, Vol. 1, Providence, Rhode Island, American Mathematical Society, 1973, pp. 80-129.

[31] The R project for statistical computing. <https://www.r-project.org/> (Accessed May 2018).

[32] R.B. D'Agostino, M.A. Stephens, (Eds), Goodness-of-fit techniques, Statistics: a series of textbooks and monographs, Marcel Dekker Inc, New York, 1986.

[33] D.B. Owen, Handbook of statistical tables, Addison-Wesley Publishing Company Inc., Massachusetts, 1962.

[34] R.E. Odeh, Critical values of the sample product-moment correlation coefficient in the bivariate normal distribution, Communications in Statistics - Simulation and Computation 11, 1982, pp. 1-26.

[35] GOST 13098:2006, Rhodium. Marks, Standardinform, Moscow.

[36] H.R. Rollinson. Using geochemical data: evaluation, presentation, interpretation, Taylor & Francis, New York, 1993.

[37] T. Vigen, Spurious correlations, Hachette Books, New York – Boston, 2015.

[38] P. Kynčlová, K. Hron, P. Filmoser, Correlation between compositional parts based on symmetric balances, Math Geosci 49/6 (2017) 777-796.

[39] F. Wang, J. Chen, Capability index using principal component analysis. Quality Engineering 11/1 (1998) 21–27.

[40] I.T. Jolliffe, Principal Component Analysis, 2nd edn., Springer Series in Statistics. Springer, New York, 2002.

[41] L. Pendrill, H. Karlson, N. Fischer, S. Demeyer, A. Allard, EURAMET: A guide to decision-making and conformity assessment - A report of the EMRP joint project NEW04 "Novel mathematical and statistical approaches to uncertainty evaluation", 2015. <http://publikationer.extweb.sp.se/ViewDocument.aspx?RapportId=29488> (Accessed May 2018).

[42] A. Buccianti, Is compositional data analysis a way to see beyond the illusion? Computers & Geosciences 50 (2013) 165-173.

[43] A. Buccianti, E. Grunsky, Compositional data analysis in geochemistry: Are we sure to see what really occurs during natural processes? Journal of Geochemical Exploration 141 (2014) 1-5.

[44] J. Bacon-Shone, A short history of compositional data analysis. In: V. Pawlowsky-Glahn, A. Buccianti, (Eds), Compositional Data Analysis. Theory and Applications, 1st edn., West Sussex, UK, Wiley, 2011, pp. 3-11.

[45] K. G. Van den Boogaart, R. Tolosana-Delgado, Analyzing Compositional Data with R, Springer-Verlag, Berlin Heidelberg, 2013.

[46] V. Pawlowsky-Glahn , J.J. Egozcue, R. Tolosana-Delgado, Modeling and Analysis of Compositional Data, Wiley Online Library, 2015, DOI: 10.1002/9781119003144.

[47] A. Gelman, J.B. Carlin, S.H. Stern, D.B. Dunson, A. Vehtari, D.B. Rubin, Bayesian Data Analysis, 3^{d} edn., Charman & Hall/CRC, Boca Raton, 2014.

[48] C. Zaiontz, Real statistics using Excel. Cholesky decomposition. <http://www.real-statistics.com/linear-algebra-matrix-topics/cholesky-decomposition/> (Accessed May 2018).

[49] I. Kuselman, F. Pennecchi, C. Burns, A. Fajgelj, P. de Zorzi, IUPAC/CITAC Guide: Investigating out-of-specification test results of chemical composition based on metrological concepts (IUPAC Technical Report), Pure Appl Chem 84 (2012) 1939-1971.

[50] B. Narasimhan, S.G. Johnson, Package 'cubature'. Adaptive multivariate integration over hypercubes, 2016. <https://cran.r-project.org/web/packages/cubature/cubature.pdf> (Accessed May 2018).

[51] A. Subaric-Leitis, Risikoanalyse Multivariater Konformitätsprüfungen. tm – Technisches Messen 77 (2010) 662-670.

Figure captions

Fig. 1. A scheme of the four-dimensional sub-domain of feasible compositions of the PtRh alloy. This is a three-dimensional simplex (each its vertex is c_i = 100 %, i = 1, 2, 4), where the feasible alloy compositions are shown as a space filled in red, while the fourth dimension of c_3 is indicated by a blue curve-pointer. The dotted lines are the specification limits truncating the simplex.

Fig. 2. **Distributions of the test results.** Histogram of the measured *i*-th component content $c_{i\mathrm{m}}$ %, and corresponding theoretical normal pdf for: a) Pt, $i = 1$; b) Rh, $i = 2$; c) the three impurities, $i = 3$; and d) the eight impurities, $i = 4$.

Fig. 3. **Total specific consumer's risk $R^*_{\mathbf{total}}$ values in dependence on the measured *i*-th component content $c_{i\mathbf{m}}$.** The $c_{i\mathrm{m}}$ values vary on their specification intervals from $T_{\mathrm{L}i}$ to $T_{\mathrm{U}i}$. The risk values are shown by line 1 versus:

a) Pt content $c_{1\mathrm{m}}$ at the Rh content $c_{2\mathrm{m}}$ in the specification interval from 7.3 to 7.7 %, and the contents of the three and the eight impurities, $c_{3\mathrm{m}} = 0.052$ % and $c_{4\mathrm{m}} = 0.059$ %, respectively; lines 2 and 3 demonstrate the sub-domain of feasible alloy compositions, respectively; dotted line 4 is for the minimum observed $c_{1\mathrm{m}}$ value, whereas line 3 coincides with the maximum observed $c_{1\mathrm{m}}$ value;

b) Rh content $c_{2\mathrm{m}}$ at $c_{1\mathrm{m}} = 100\ \% - c_{2\mathrm{m}} - c_{4\mathrm{m}}$, $c_{3\mathrm{m}} = 0.052$ %, and $c_{4\mathrm{m}} = 0.059$ %; lines 2 and 3 show the interval of observed $c_{2\mathrm{m}}$ values;

c) content $c_{3\mathrm{m}}$ of the three precious impurities at $c_{1\mathrm{m}} = 100\ \% - c_{2\mathrm{m}} - c_{4\mathrm{m}}$, $c_{2\mathrm{m}} = 7.46$ % and $c_{4\mathrm{m}} = 1.16\ c_{3\mathrm{m}}$; lines 2 and 3 show the interval of observed $c_{3\mathrm{m}}$ values;

d) content $c_{4\mathrm{m}}$ of the eight impurities at $c_{1\mathrm{m}} = 100\ \% - c_{2\mathrm{m}} - c_{4\mathrm{m}}$, $c_{2\mathrm{m}} = 7.46$ % and $c_{3\mathrm{m}} = c_{4\mathrm{m}}/1.16 \leq 0.12$ %; lines 2 and 3 show the interval of observed $c_{4\mathrm{m}}$ values .

Fig. 4. **Surface of $R^*_{\mathbf{total}}$ vs. Rh measured content $c_{2\mathbf{m}}$ and measured content $c_{4\mathbf{m}}$ of the eight impurities.** The plot in Fig. 4a is for the four-component scenario at $c_{3\mathrm{m}} = c_{4\mathrm{m}}/1.16$, but not exceeding 0.12 %, and $92.2\ \% \leq c_{1\mathrm{m}} = 100\ \% - c_{2\mathrm{m}} - c_{4\mathrm{m}} \leq 92.8\ \%$. The second plot, in Fig. 4b, shows the surface of the risks R^*_{total} for the two-component scenario, when $c_{1\mathrm{m}}$ and $c_{3\mathrm{m}}$ are not taken into account as strongly correlated with $c_{2\mathrm{m}}$ and $c_{4\mathrm{m}}$, respectively. A color column bar gives indication of the risk values between the minimum and the maximum on the surface. The same scale of the risk axis from 0 to 1 is used in both the Fig. 4 plots, but each color bar refers to its plot only.

Novelty Statement

An alloy is considered as a multicomponent material with complex correlations among contents of its components. Evaluation of a total risk of a false decision on conformity of an alloy due to measurement uncertainty and correlation of test results is developed. Studying test results of a PtRh alloy, it was shown that simplification of the testing by reducing the number of the components under control, from strongly correlated to those which are practically uncorrelated, leads to a significant increase of the total (global) risk.

Table 1. Standard measurement uncertainties of the impurities

Impurity	m_{imp}, %	s_{imp}, %	Δ, %	u	
				Symbol	Value, %
Pd	0.048	0.018	0.016	u_{Pd}	0.008
Ir	0.0038	0.0036	0.0015	u_{Ir}	0.0008
Au	< 0.0030	< 0.0030	0.0011	u_{Au}	0.0006
Fe	0.0071	0.0052	0.0028	u_{Fe}	0.0014
Pb	< 0.0003	< 0.0003	0.0002	u_{Pb}	0.0001
Si	< 0.0005	< 0.0005	0.0003	u_{Si}	0.0002
Sn	< 0.0003	< 0.0003	0.0002	u_{Sn}	0.0001
Zn	0.0003	0.0002	0.0002	u_{Zn}	0.0001

Note: m_{imp} and s_{imp} are the mean and the standard deviation, respectively, of the measurement results of the impurity mass fractions, %; symbol < is used with the limit of detection (LOD) as 'less than LOD'; Δ is the value equal to the expanded measurement uncertainty at coverage factor 1.96 and normal distribution; and u is the standard measurement uncertainty.

Table 2. Parameters of the distributions of the test/measurement results c_{im}

Component	Index	Parameter		
	i	m_i , %	s_i , %	D_i
Pt	1	92.483	0.081	0.063
Rh	2	7.457	0.073	0.064
Three impurities	3	0.052	0.019	0.094
Eight impurities	4	0.059	0.021	0.086

Note: m_i is the mean, and s_i - the standard deviation; D_i - the maximal absolute difference between empirical and theoretical cumulative distribution functions.

Table 3

Table 3. Pearson's correlation coefficients r_{ij} of test results

Component	Index	Pt	Rh	Three impurities	Eight impurities
	i \ *j*	1	2	3	4
Pt	1	1	-0.967	-0.469	-0.467
Rh	2		1	0.239	0.228
Three impurities	3			1	0.970
Eight impurities	4				1

Figure 1

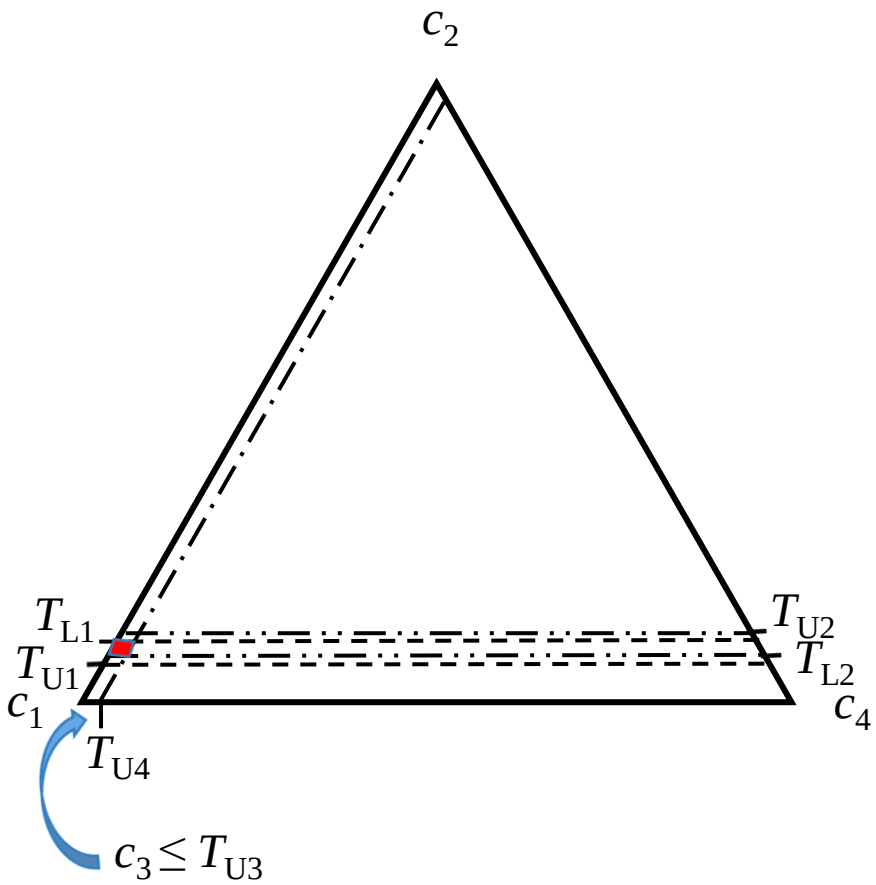

Figure 2

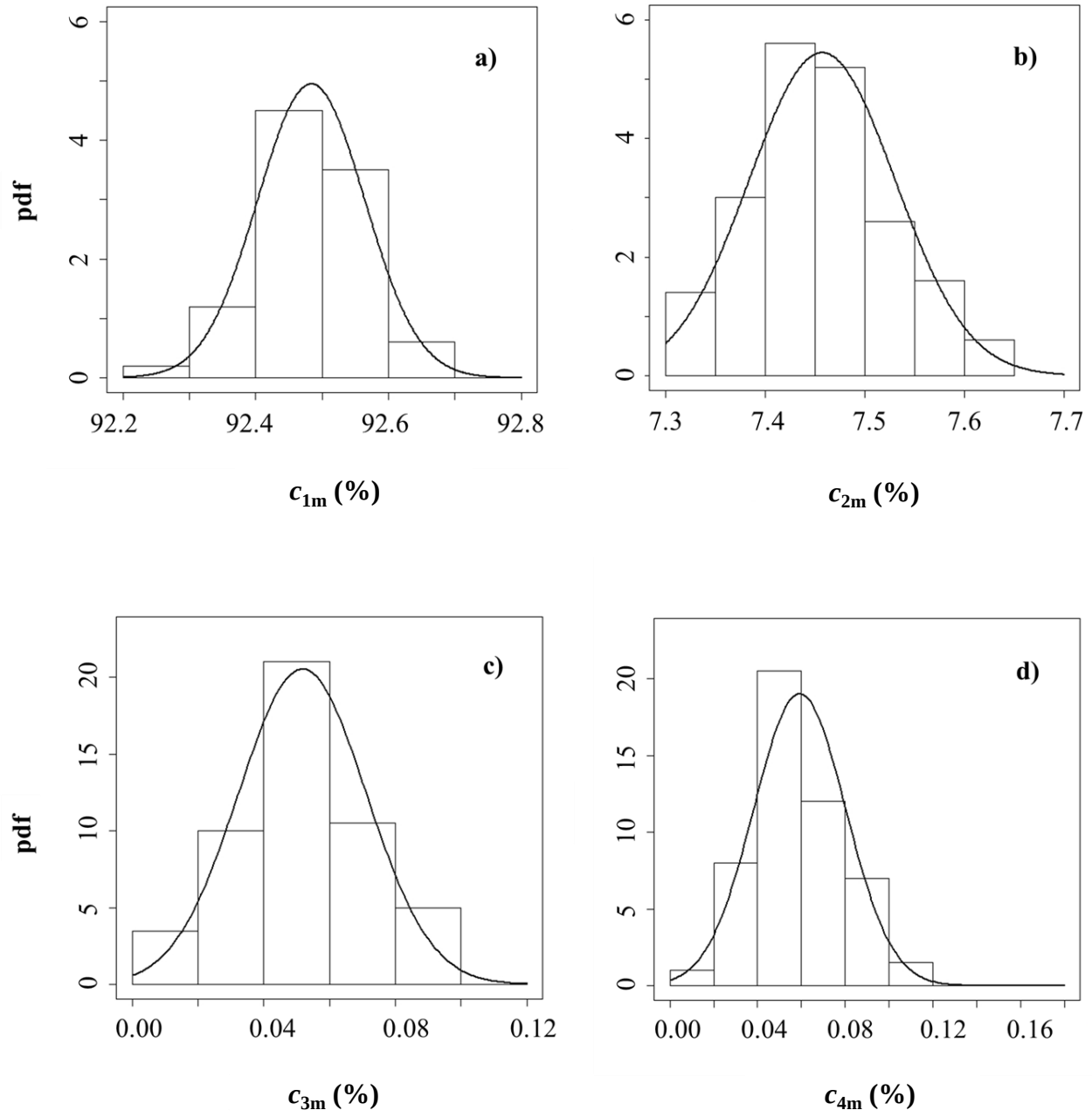
a)
b)
c)
d)
pdf
pdf
0
2
4
6
0
5
10
15
20
92.2
92.4
92.6
92.8
7.3
7.4
7.5
7.6
7.7
0.00
0.04
0.08
0.12
0.00
0.04
0.08
0.12
0.16
c_{1m} (%)
c_{2m} (%)
c_{3m} (%)
c_{4m} (%)

Figure 3

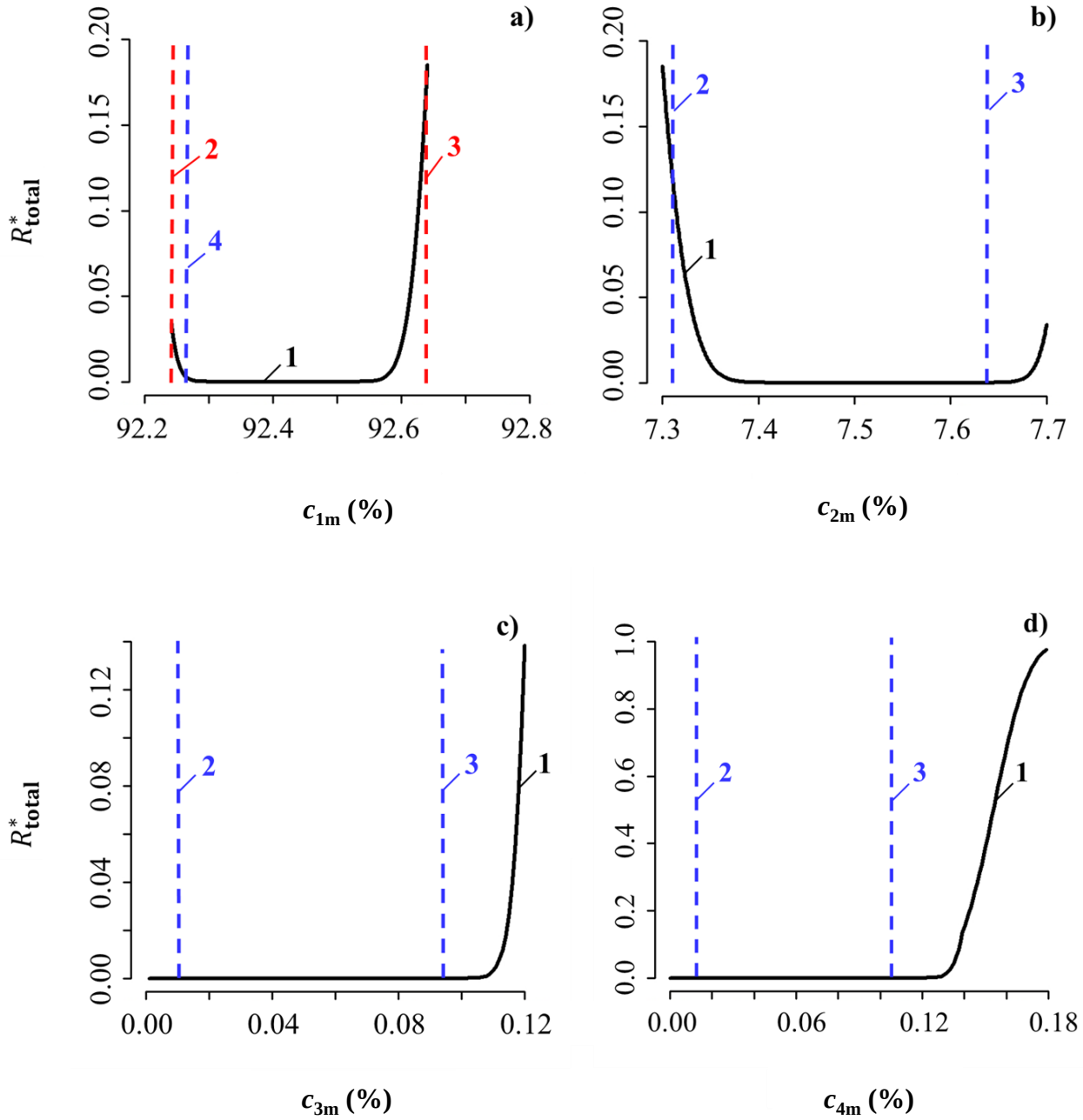
a)
b)
c)
d)
R^*_{total}
c_{1m} (%)
c_{2m} (%)
c_{3m} (%)
c_{4m} (%)
1
2
3
4
0.00
0.05
0.10
0.15
0.20
92.2
92.4
92.6
92.8
7.3
7.4
7.5
7.6
7.7
0.04
0.08
0.12
0.06
0.18
0.0
0.2
0.4
0.6
0.8
1.0
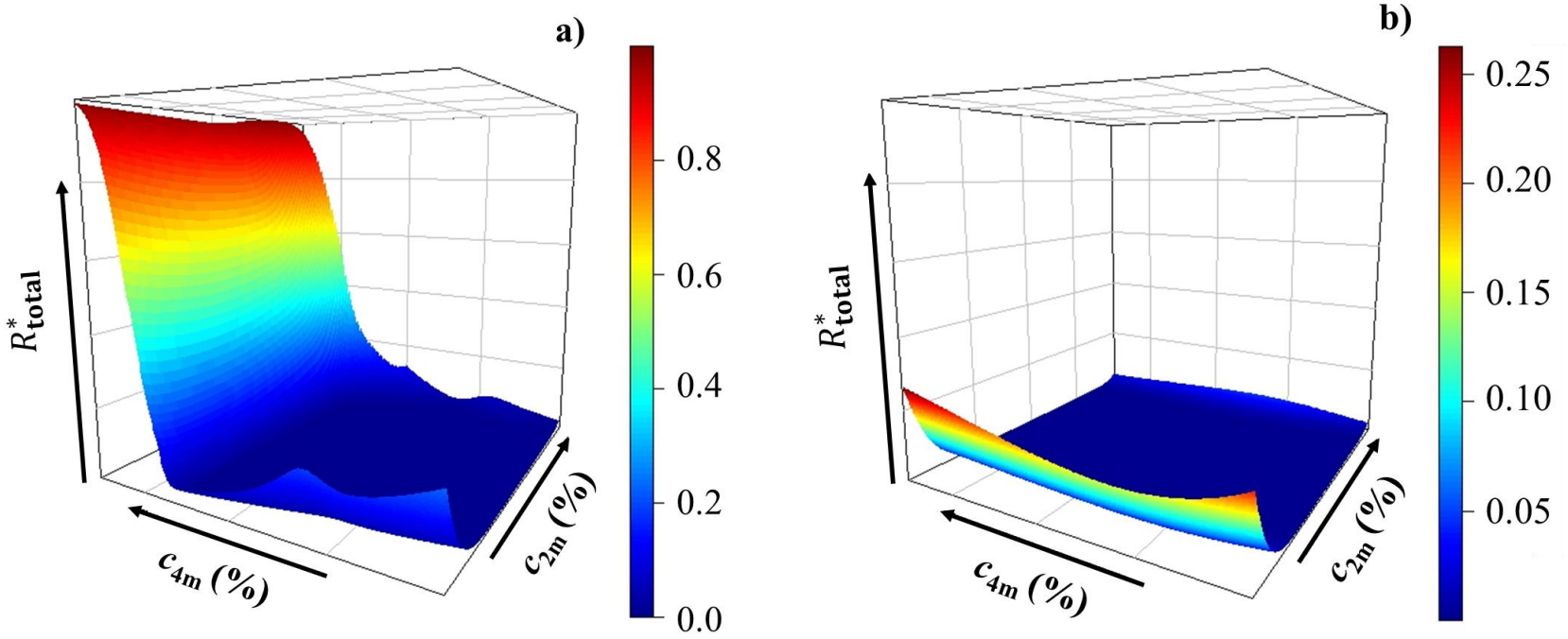
Figure 4